DOI 10.1007/s11015-018-0685-z
Metallurgist, Vol. 62, Nos. 5–6, September, 2018 (Russian Original Nos. 5–6, May–June, 2018)

FORMS OF ZINC FOUND IN ELECTRIC STEEL SMELTING FURNACE GAS CLEANING DUST

S. N. Tyushnyakov,[1] E. N. Selivanov,[2] and A. A. Pankratov[3]

UDC 669.01:669.054.8

Results are provided for a study of the elemental and phase composition of PAO Northern Pipe Plant electric steel smelting furnace gas cleaning dust. Dust particle shape and size are evaluated. X-ray microanalysis is used to determine the elemental composition of dust particles art local sampling points. It is shown that zinc in dust is found predominantly in calcium and magnesium ferrites, and also in spinels.

Keywords: furnace, steel, gas-cleaning dust, composition, structure, size, phases, iron oxides, zinc ferrite, formation mechanism.

Currently there is an increase in the proportion of metal scrap introduced into steel melting unit charges with a high nonferrous metal content, including zinc [1, 2]. Heating and melting of steel scrap containing zinc leads to zinc evaporation [2]. A number of elements and compounds volatilize in the high-temperature zone (above 3500 ºC) of an electric furnace and are transferred into sublimates. In an oxidizing gas atmosphere zinc metal vapor is oxidized to ZnO and leaves the furnace. During electric melting of scrap almost all of the zinc is transferred into a dust and gas stream and thereby separated from the finished metal. In a dust and gas stream there is a high probability of forming complex compounds, for example zinc ferrite $ZnFe_2O_4$.

In a gas cleaning system mechanically entrained particles, condensed metals, and compounds, and also their reaction products, are captured in the form of dust and slurry. In contrast to blast furnace dust [3–5] the fine products captured in a steel melting unit dust and gas cleaning system have a smaller size and carbon content. According to data in [2, 3] the chemical composition of dust and slurry of steel melting units vary over wide limits, wt.%: 32.0–67.7 Fe_{tot}, 2.3–19.7 FeO, 48.3–66.0 Fe_2O_3, 1.0–12.0 SiO_2, 1.5–22.1 CaO, 0.1–20.3 ZnO, 0.5–4.0 C, 0.1–0.7 S.

The microstructure and shape of end product metals (zinc and iron) in dust of a gas cleaner mainly determines the efficiency of their treatment technology. Pyrometallurgical methods for dust treatment and slurry of steel smelting gas cleaning units have been considered in [2, 6–10]. Data are provided in [11–13] for thermodynamic modeling of pyrometallurgical reduction and chlorination in order to extract valuable metal from EAF dust.

During development of treatment for finely dispersed materials a study of their chemical and phase composition is limited [9, 10], and the microstructure of dust and slurry from gas cleaners, in particular Ural enterprises, remains little studied. The aim of the present work is to study the microstructure, chemical, and phase composition of gas cleaning dust from electric steel smelting furnaces, which is a basis for further development of their utilization technology.

[1] FGBUN Institute of Metallurgy, Ural Section, Russian Academy of Sciences, Ekaterinburg, Russia; e-mail: tyushnyakov.sn@gmail.com.
[2] FGBUN Institute of Metallurgy, Ural Section, Russian Academy of Sciences, Ekaterinburg, Russia; e-mail: pcmlab@mail.ru.
[3] FGBUN Institute of High-temperature Electrochemistry, Ural Section, Russian Academy of Sciences, Ekaterinburg, Russia; e-mail: A.Pankratov@ihte.uran.ru.

Translated from Metallurg, Vol. 62, No. 6, pp. 8–13, June, 2018. Original article submitted August 16, 2017.

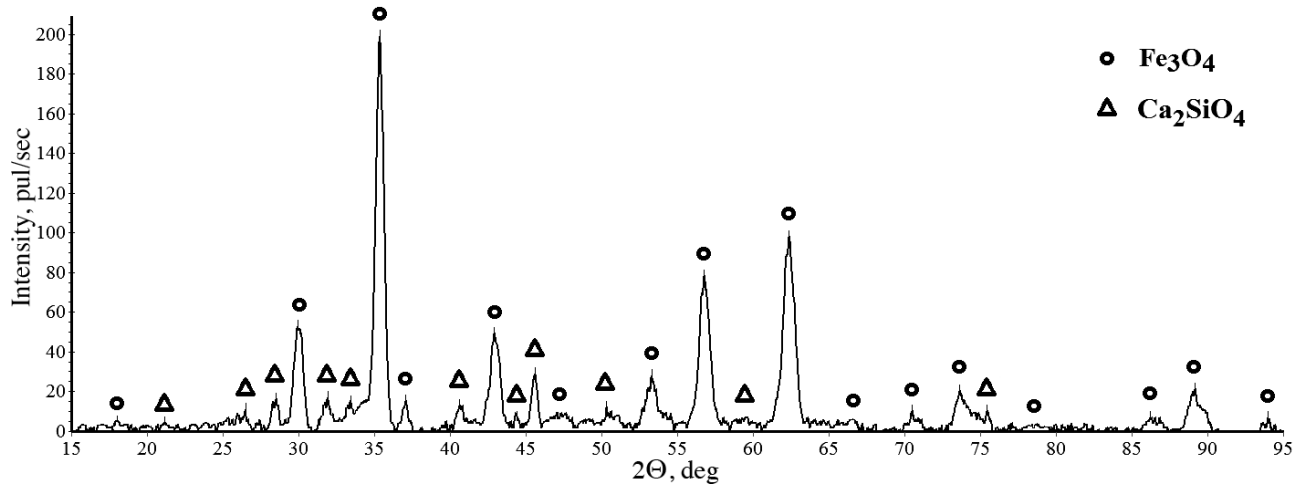

Fig. 1. Gas-cleaning dust diffraction pattern.

Research Procedure

Grain size composition was studied using a HORIBA LA-950 particle size laser analyzer. X-ray phase analysis (XPA) was conducted in an automatic DRON-2.0 diffractometer (graphite monochromator in the emerging beam; Cu K_α radiation) and in order to identify phases a PDF-2 (powder Diffraction File) database was used. X-ray microanalysis (XMRA) was performed in a JSM-5900LV scanning electron microscope and an energy-dispersion X-ray microscope Oxford INCA Energy 200. The procedure of microsection preparation for microanalysis included mixing dust with epoxy resin, molding a specimen in a frame, and polishing after hardening. Before carrying out XMRA a current conducting coating of electrical conducting powder was deposited at a microsection surface.

The initial specimen taken was dust from bag filters (moisture content 0.6%) EAF-135 (PAO Northern Pipe Plant) containing wt.%: 4.5 Zn; 41.2 Fe_{tot}, 4.9 Mn, 9.0 Ca, 1.5 Mg, 2.6 Si, 0.5 Al, 2.8 C, 0.7 S, 2.0 Cl, 0.2 F.

Research Results

According to XPA data (Fig. 1) dust specimens contain iron oxide Fe_3O_4 and calcium orthosilicate Ca_2SiO_4. Some shift in iron oxide and calcium orthosilicate reflections compared with pure substances is caused by formation of solid solutions, for example, FeO_x–ZnO, FeO_x–MnO, FeO_x–CaO and CaO–SiO_2–FeO_x, and also presence of impurities distorting the primary (mechanical entrainment of charge) and secondary (phase formation during cooling) minerals [15].

According to grain size analysis data (see Fig. 2), dust is represented by a considerable amount of finely dispersed (to 10 μm) particles. The average particle size d_{av} = 3.6 μm, and the median M_d = 2.2 μm. The small size of dust particles predetermines the precision of subsequent instrument measurements of particle composition.

It follows from XMRA data and characteristic radiation of elements (Fig. 3) that a specimen is represented by iron oxides, calcium ferrite, and phases that may be classified as manganese and zinc ferrites. Individual particles with increased silicon and calcium content are also encountered.

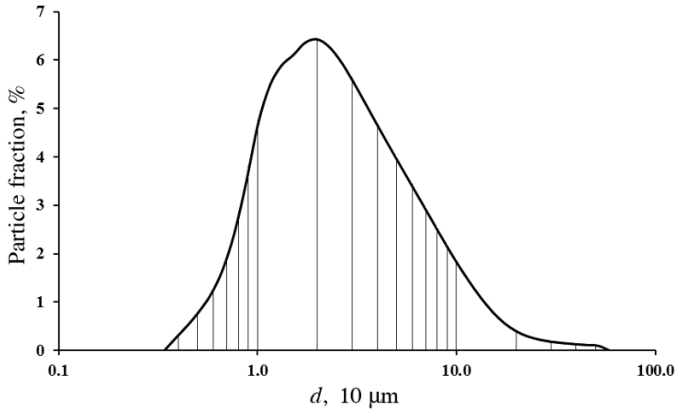

Fig. 2. Gas cleaning dust grain size composition.

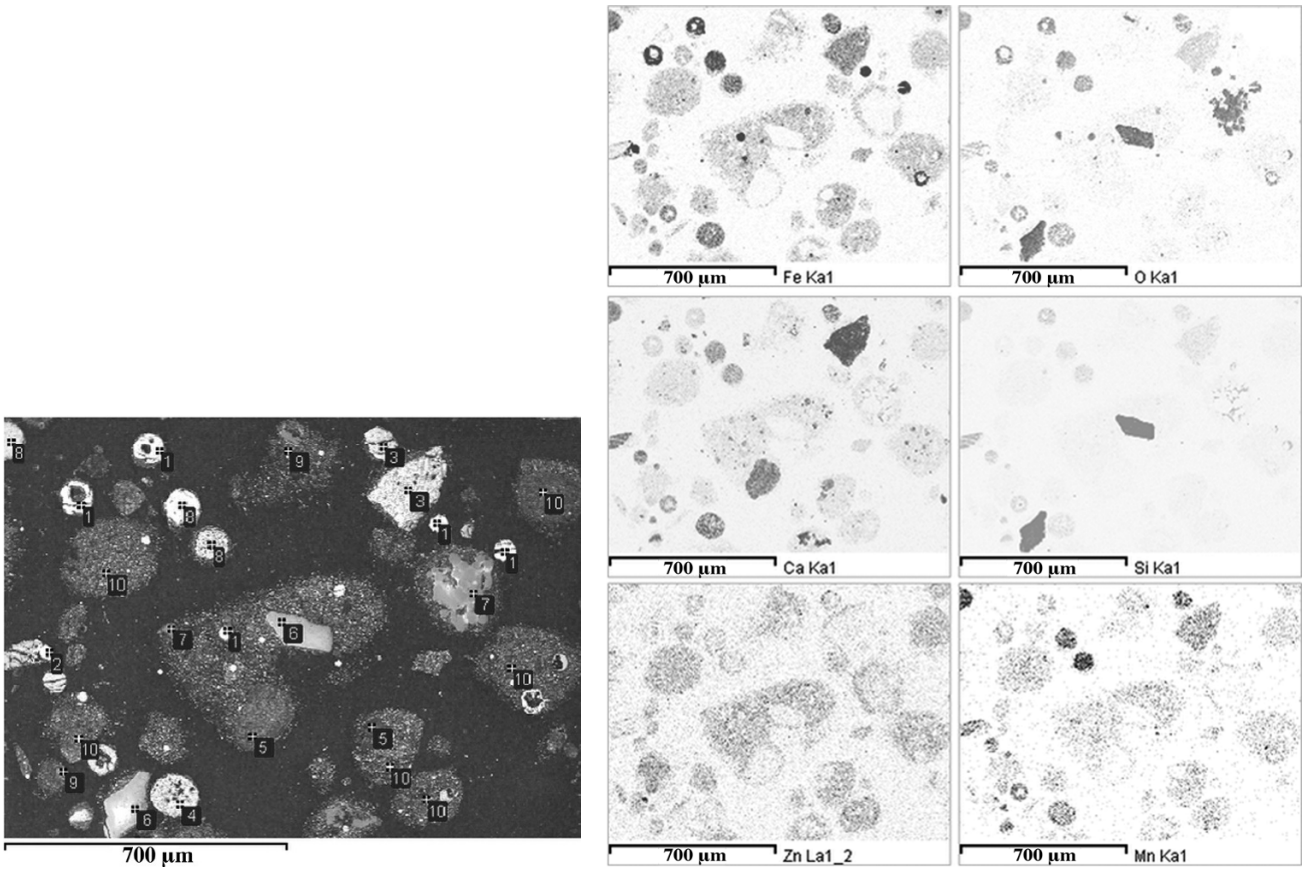

Fig. 3. Gas cleaning dust specimen microstructure (a) and particle shape in element characteristic radiation (b).

With respect to shape all of the dust particles may be conditionally separated into three groups: irregular shape with size up to 200 μm, rounded shape with size 10–80 and up to 10 μm. Particles of irregular shape are represented by flux and scale fragments, mechanically entrained by the gas stream. In such specimens silicon, calcium, and magnesium oxides were observed as fine heat treated fragments of flux, used in the steel melting processes.

Table 1
Dust Specimen Composition at Local Sampling Points

Point number	Phase	Content, wt.%									
		Fe	Zn	Mg	Si	Ca	Mn	Al	Cl	O	S
1	Fe_2O_3	54.7–68.3	–	0.8–1.3	1.2–4.1	0.8–2.8	0.6–1.4	up to 2.0	–	30.9–39.4	–
2	Center — Fe; surface — Fe_2O_3	93.8	–	–	0.3	–	–	–	–	5.9	–
3	$Ca_{1,7}Fe_2O_{4,7}$–$Ca_{3,3}Fe_2O_{6,3}$	23.7–34.2	–	1.1–3.1	2.4–4.1	21.3–28.2	3.6–6.8	0.6–2.9	–	26.9–40.3	–
4	$Ca_{2,4}Fe_{1,4}SiO_{6,5}$	20.6	–	0.5	9.1	30.9	1.3	1.8	–	34.9	0.5
5	CaO	–	–	–	up to 1.2	31.6–34.2	–	–	0.8–2.2	63.0–64.2	–
6	SiO_2	–	–	–	33.3–35.4	–	–	–	–	64.6–66.7	–
7	MgO	0.3–1.2	–	53.6–60.1	–	–	–	–	–	38.7–46.0	–
8	$Ca_{0,6}Fe_2Si_{0,4}O_{4,4}$–$Ca_2Fe_2SiO_{5,8}$	22.9–43.7	–	2.0–4.6	4.0–8.2	8.5–16.4	4.7–7.0	1.4–2.5	–	33.4–38.7	–
9	$Zn_{0,4}Mn_{0,3}Fe_2O_{3,9}$–$Zn_{0,6}Mn_{0,6}Fe_2O_{4,5}$	29.6–40.6	8.5–11.0	1.6–4.6	2.9–3.4	3.0–3.1	5.4–9.4	0.4–0.7	0.0–1.6	34.0–36.8	0.6–0.8
10	$Ca_{0,3}Fe_2O_{3,3}$–$CaFe_2O_4$	28.3–46.2	2.2–5.1	1.5–4.3	3.3–5.5	5.4–11.6	1.9–9.2	up to 0.6	1.6–2.8	30.2–50.1	1.1–1.3

Concerning coarse (10–80 μm) round particles, they have an internal metal nucleus and an oxidized surface. In some particle the iron content reaches 93.8%. It is apparent that during steel melting fine droplets of iron metal are carried over by the exhaust gas stream. Cooling of these droplets in a gas stream leads to partial surface oxidation and therefore the average oxygen content in particles reaches 5.9%. Finer (up to 10 μm) dust particles are probably a condensed product forming in the course of action of a low-temperature plasma on condensed and sublimated metal in the furnace space beneath the arch.

In a microsection of a dust specimen the main area is occupied by particles of calcium ferrite of complex composition containing zinc and manganese. Particles of iron (III) oxide are revealed, containing up to wt.%: 1.3 Mg, 2.0 Al, 4.1 Si, 2.8 Ca, 1.4 Mn (Table 1). Iron-calcium silicates may be separated into two types: the first corresponds to the formula $Ca_{2.4}Fe_{1.4}SiO_{6.5}$ and has a small content of such impurities as magnesium (0.5%), aluminum (.18%, manganese (1.3%) and sulfur (0.5%); the second composition from $Ca_{0,6}Fe_2Si_{0,4}O_{4,4}$ to $Ca_2Fe_2SiO_{5,8}$ differs in an increased manganese content (up to 7.0 wt.%), manganese (2.0–4.6%), and aluminum (1.4–2.5%).

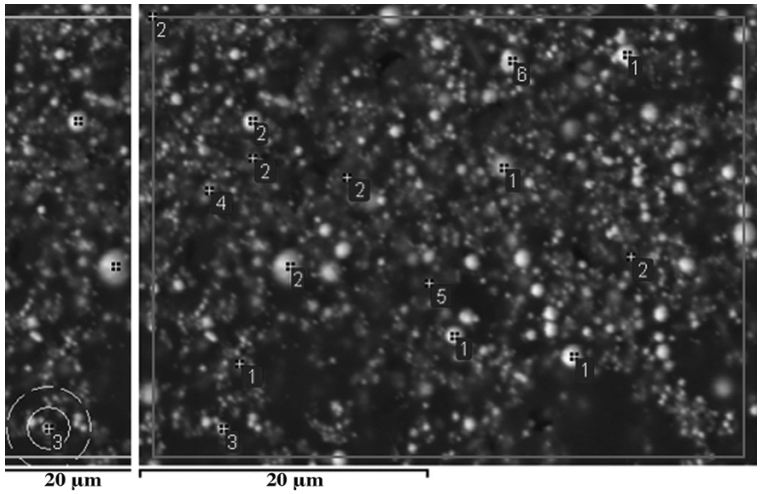

Fig. 4. Microstructure of dust particles with size less than 2 μm.

Conglomerates of ferrite particles with a size of 80–100 μm have been revealed in a dust specimen. These conglomerates were probably formed as a result of particle contact in the dust catching unit. Their composition corresponds calcium ferrite of non-stoichiometric composition $Ca_{1,7–3,3}Fe_2O_{4,7–6,3}$ with an impurity content, wt.%: 1.1–3.1 Mg, 0.6–2.9 Al, 2.4–4.1 Si, 3.6–6.8 Mn. Within the field of a microsection an extensive region is occupied by particles (conglomerates) whose phase composition may be identified as calcium ferrites of variable composition $Ca_{0,3–1,0}Fe_2O_{3,3–4,0}$. In these phase the main impurity elements are zinc (5.1%), and also sulfur (1.1–1.3%) and chlorine (1.6–2.8%). The source of sulfur and chlorine in dust is organic impurities (oil, plastics, etc.) entrained in a charge with metal scrap. Presence within an electric melting charge composition of chlorine-containing compounds provides the possibility of occurrence chloride sublimation. As is well known [16, 17], chlorine- and fluorine-containing compounds with an increase in temperature form metal chlorides ($FeCl_3$, etc.) readily volatilized and transferred into the gas phase. According to data in [18], the boiling temperature for $ZnCl_2$ is 732 ºC, for $FeCl_2$ it is 1012 ºC, and for $FeCl_3$ it is 315 ºC. At steel smelting process temperatures iron and zinc chlorides volatilize and then during cooling of a dust and gas stream in cleaning units they condense on the form of independent phase, including on dust particles.

In gas cleaning dust phases are detected of manganese-zinc ferrites of variable composition $Zn_{0,4–0,6}Mn_{0,3–0,6}Fe_2O_{3,9–4,5}$, containing up to 9.4% Mn and 11.0% Zn. The impurities detected in these ferrite are magnesium (1.6–4.6%), silicon (2.9–3.4%), calcium (3.0–3.1%), aluminum (up to 0.7%), chlorine (up to 1.6%), and sulfur (up to 0.8%). Formation of these ferrites is explained by the composition of the raw material treated, metal sublimation, their combined cooling and oxidation. An increase should be noted in the manganese and zinc content in this ferrite, which predetermines the choice of technology for subsequent zinc separation.

At high magnification numerous spheroidal fragments (Fig. 4) 0.5–2 μm in diameter are revealed, represented by iron oxide containing impurities, wt.%: 0.9–6.7 Zn, 1.2–6.6 Mn, 0.6–7.8 Ca, 1.9–2.6 Na, 0.6–2.4 Mg, 0.7–4.2 Si, 0.3–1.7 Cl (Table 2). Formation of spheroidal particles is possible both as a result of dust entrainment of fine metal droplets with subsequent oxidation, and also with condensation of metal or its oxide from vapor. Assuming that within the arc zone a charge and melt are subjected to action of a low-temperature plasma (≈ 3500 ºC), formation of particles of this shape should be considered as a condensation product from vapor [19–23].

Some dust particles with diameter of about 1 μm have been identified as calcium ferrites of composition varying over a wide range, i.e., from $Ca_{0.6}Fe_2O_{3.6}$ to $Ca_{2.3}Fe_2O_{5.3}$. Ferrites have an increased content of zinc

Table 2
Dust Particle Composition at Sampling Points (see Fig. 4)

Point number	Phase	Content, wt.%								
		Fe	Zn	Mg	Si	Ca	Mn	Na	Cl	O
1	Fe_2O_3	37.7–58.6	0.9–6.7	0.6–2.4	0.7–4.2	0.6–7.8	1.2–6.6	1.9–2.6	0.3–1.7	33.7–37.2
2	$Ca_{0,6–2,3}Fe_2O_{3,6–5,3}$	26.9–42.0	up to 9.4	1.7–3.8	1.0–3.7	8.8–25.1	3.3–7.2	–	up to 5.9	26.4–48.9
3	$Ca_{0,4}Mn_{0,5}Fe_2O_{4,2}$	32.7	2.3	4.6	2.8	5.0	8.2	3.1	2.5	38.1
4	$Ca_{0,5}Zn_{0,4}Fe_2O_{3,9}$	38.8	9.0	1.7	3.8	6.7	3.9	–	2.6	31.5
5	$Ca_{0,6}Na_{1,1}Fe_2O_{4,2}$	31.7	2.6	2.0	5.1	6.9	3.9	7.4	3.0	31.7
6	$Zn_{0,6}Mn_{0,6}Fe_2Si_{1,2}O_{6,9}$	30.0	11.3	1.6	8.8	2.2	9.1	–	0.8	34.6

(up to 9.7%), manganese (up to 7,2%), and chlorine (up to 5.9%). Individual calcium ferrite particles are observed containing impurities of manganese (8.2%), zinc (9.0%) and sodium (7.4%). In manganese-calcium ferrite the probable phase composition is close to $Ca_{0,4}Mn_{0,5}Fe_2O_{4,2}$, also containing (wt.%) 3.1 Na, 4.6 Mg, 2.8 Si, 2.5 Cl, 5.0 Ca, 2.3 Zn. The composition of the calcium ferrite is described by a formula $Ca_{0,5}Zn_{0,4}Fe_2O_{3,9}$, and the magnesium content within it reaches 1.7%, silicon 3.8%, chlorine 2.6%, and manganese 3.9%. Particles of zinc-manganese iron silicate compound have been detected with a probable phase composition $Zn_{0,6}Mn_{0,6}Fe_2Si_{1,2}O_{6,9}$, within which the zinc content comprises 11.3% and manganese 9.1%.

The mechanism of fine dust particle formation in the course of electric melting may be presented in the form of successively occurring processes of evaporation, condensation, oxidation, and quenching. Initially sublimate ($t > 3500$ °C) from a plasma zone enter into the furnace space beneath the arch ($t \approx 1100–1150$ °C) where it is cooled and mixed with air entering due to rarefaction, created by an exhaust fan through furnace leakage (body–arch, economizers–electrodes, sight windows, holes, etc.). The atmosphere created as a result of entry of air into the furnace leads to partial oxidation of a metal charge. Oxidized metal is slagged with fluxes (Cao, MgO, SiO_2) and transferred into slag. Maintenance of the required rarefaction beneath the furnace arch prevents unorganized discharge of gas into the furnace atmosphere and facilitates observation of LPC standards for harmful substances. Excess rarefaction increases the amount of air entering a furnace and consequently metal oxidation and dust entrainment. An increased amount of air entering a furnace to additional heat loss in waste gases, which increase electrical energy consumption for a unit of production.

Then electric furnace gases enter into a cleaning unit, where there is cooling to 200–400 °C. A high rate of dust and gas stream and a temperature gradient corresponds to quenching of solid particles and stabilization of non-equilibrium compositions with respect to gas oxidation potential.

An increased content of dust of such metals as iron, zinc, magnesium, and manganese points to preferred sublimation, connected with a high proportion of metal (Fe) in the high-temperature zone and vapor (Zn, Mg, Mn) partial pressure. Evaporation of metal chlorides and fluorides facilitates an increased halogenide content introduced into a charge in the form of fluxes (CaF_2) and inorganic impurities (plastics, oil, etc.).

The information obtained about the structure and composition of dust makes it possible to draw conclusions about possible methods for their utilization. Use of direct hydrometallurgical treatment of dust is incorrect,

since use of dilute acid solution does not make it possible to transfer zinc into solution from the ferrites revealed. It is preferable to use technology [24] for zinc and chloride extraction from dust from eclectic furnace gas cleaners by two-stage Waelz treatment followed by use of products for the final purpose.

CONCLUSIONS

Bag filter dust of steel melting gas cleaning bag filters of PAO STZ steel melting furnaces is represented by finely dispersed spheroidal particles (0.4–51.5 μm), i.e., a product of condensation and oxidation of metal vapor and charge fragments mechanically entrained by the gas stream. The main phase dust components are iron oxides, iron-calcium silicates, manganese-zinc ferrites and other compounds with impurities of zinc, magnesium, silicon, chlorine, and sulfur. Zinc is predominantly revealed in the form of complex ferrites (size up to 2 μm).

The data obtained may be used for developing technology for utilizing zinc-containing dust for metallurgical conversion gas cleaners.

Work was carried out within the scope of an IMET UrO RAN state assignment on theme No. 0396–2015–0082 (registration No. AAAA-A16–116022610056–0).

REFERENCES

1. V. A. Kudrin, *Steel Production Theory and Technology* [in Russian], Mir, Moscow (2003).
2. A. V. Tarasov, A. D. Besser and V. I. Mal'tsev, *Metallurgical Processing of Secondary Zinc Raw Material* [in Russian], Gintstsvetmet, Moscow (2004).
3. S. M. Andon'ev and O. V. Filip'ev, *Ferrous Metallurgy Dust and Gas Discharges* [in Russian], Metallurgiya, Moscow 91979).
4. I. N. Tanutrov, E. N. Selivanov, and S. N. Tyushnyakov, "Prospects for using direct current furnaces for processing slag of autogenic melting of copper concentrates and ferrous metallurgy slurries," *Tsvet. Met.*, No. 4, 43–47 (2012).
5. S. N. Tyushnyakov, E. N. Selivanov, and V. M. Chumarev, "Evaluation of the zinc sublimation rate from slag in a direct current furnace," *Tsvet. Met.*, No. 12, 13–17 (2013).
6. M. A. Abdel-latif, "Fundamentals of zinc recovery from metallurgical wastes in the Enviroplas process," *Minerals Engineering*, **15**, No. 11, 845–952 (2002).
7. A. Fleischanderl, U. Gennari, and A. Ilie, "ZEWA — metallurgical process for treatment of residues from steel industry and other industrial sectors to generate valuable products," *Ironmaking and Steelmaking*, **31**, No. 6, 444–449 (2004).
8. S. A. Yakornov, A. M. Pan'shin, P. A. Kozlov, and D. A. Ivakin, "Contemporary state of electric arc furnace dust treatment," *Tsvet. Met.*, No. 4, 23–29 (2017).
9. N. V. Nemchinova, V. E. Chernykh, A. A. Tyutrin, and A. E. Patrushov, "Treatment of electric steel melting furnace production dust with the aim of extracting zinc and iron," *Stal'*, No. 5, 68–72 (2016).
10. P. I. Grudinskii, V. P. Korneev, V. G. Lyubanov, et al., "Electric arc furnace dust — prospective material for producing nonferrous metals ad cast iron," *Perspekt. Materialy*, No. 10, 69–75 (2016).
11. C. A. Pickles, "Thermodynamic modelling of the multiphase pyrometallurgical processing of electric arc furnace dust," *Minerals Engineering*, **22**, 977–985 (2009).
12. C. A. Pickles, "Thermodynamic analysis of the selective carbothermic reduction of electric arc furnace dust," *J. Hazardous Materials*, **150**, 265–278 (2008).
13. C. A. Pickles, "Thermodynamic analysis of the selective chlorination of electric arc furnace dust," *J. Hazardous Materials*, **166**, 1030–1042 (2009).
14. I. E. Doronin and A. G. Svyazhin, "Steel smelting unit dust and slurry as a raw material for producing zinc and steel," *Izv. Vyssh. Uchebn. Zaved., Tsvet. Met.,* No. 5, 31–35 (2012).
15. *Powder Diffraction File (PDF), Produced by the International Centre for Diffraction Data*, Newtown Square, PA, USA (2012), No. 01–075–1372; No. 01–076–3610.
16. I. S. Morozov, *Use of Chlorine in Metallurgy of Rare and Nonferrous Metals* [in Russian], Nauka, Moscow (1966).
17. N. P. Lyakishev (editor), *Encyclopaedic Dictionary for Metallurgy, in 2 Vol.* [in Russian], Intermet Inzhiniring, Moscow (2000).

18. A. I. Efimov, L. P. Belorukova, I. V. Vasil'kova, and V. P. Chechev, *Properties of Inorganic Compounds* [in Russian], Khimiya, Leningrad (1983).
19. S. S. Naboichenko, O. S. Nichiporenko, I. B. Murashova, et al., *Nonferrous Metal Powders — Handbook* [in Russian], Metallurgiya, Moscow (1997).
20. I. V. Frishberg, S. V. Gribovskii, E. S. Korepanova, and A. I. Okunev, "Preparation of zinc powder during metallothermic reduction of zinc raw material," *Zv. Akad. Nauk SSSR, Metally,* No. 4, 53–55 (1973).
21. L. Zhan, X. Xiang, B. Xie, and B. Gao, "Preparing lead oxide nanoparticles from waste electric and electronic equipment by high temperature oxidation-evaporation and condensation," *Powder Technology*, **308**, 30–36 (2017).
22. X. Xiang, F. Xia, L. Zhan, and B. Xie, "Preparation of zinc nano structured particles from spent zinc manganese batteries by vacuum separation and inert gas condensation," *Separation and Purification Technology*, **142**, 227–233 (2015).
23. A. V. Sazonov, É. É. Merker, and A. A. Kozhukov, "Questions of the reduction of metal evaporation intensity in high-temperature zones of contemporary AEF in the oxidation period," *Élektrometallurgiya*, No. 7, 34–39 (2017).
24. P. A. Kozlov, "Assimilation of metallurgical production waste recycling technology," *Tsvet. Met.*, No. 2, 45–52 (2014).